Open-Path, Near-Infrared Tunable Diode Laser Spectrometer for Atmospheric Measurements of H_2O

Randy D. May
Jet Propulsion Laboratory
California Institute of Technology
4800 Oak Grove Drive
Pasadena, CA 91109

Abstract. A new instrument for *in-situ* measurements of atmospheric water vapor from aircraft platforms has been developed based upon near-infrared tunable diode laser sources operating near 1.37 μm. The spectrometer features an unique open-path, multipass (Herriott) cell for true *in-situ* monitoring of water vapor concentrations with precision levels exceeding those of Lyman-α and frost-point hygrometers. External sampling outside of the aircraft boundary layer minimizes ambiguities in the measured water vapor abundances. Variable spectrum acquisition rates up to 10 Hz provide fast temporal resolution free from sampling or flow rate limitations. In its current configuration the instrument operates from the right wing pod of the NASA ER-2 research aircraft, and is optimized for measurements in the upper troposphere and stratosphere (to 20 km). Measurement precision is ±0.05 ppmv in the stratosphere for a 2s measurement integration period. The flight-ready instrument weight is 18 pounds, and power consumption, exclusive of structural heaters, is 7.5W.

1. Introduction

Water vapor plays a variety of important roles in the Earth's atmosphere. In the stratosphere and upper troposphere, H_2O abundances affect both radiative forcing and ozone levels. In the troposphere, water vapor is a primary determinant of cloudiness which controls radiative equilibrium and cooling rates in the atmosphere, and it is also the most important greenhouse gas [*Manabe and Wetherald*, 1967; *Jones and Mitchell*, 1991]. Understanding the control of water vapor is crucial to improving our understanding of the effects of aircraft emissions on climate. Water vapor is also a good tracer of transport in the lower stratosphere because of the long chemical lifetime (years), and observations of seasonal and hemispheric variations in stratospheric and upper tropospheric water vapor reinforce the need for accurate *in-situ* measurements over wide latitude regions to improve the predictability of global circulation models [*Jones and Mitchell*, 1991].

To date the majority of *in-situ* H_2O measurements made from aircraft and balloon platforms have been carried out using Lyman-α spectrometers, or frost point hygrometers. Lyman-α spectrometers infer H_2O concentrations from quantitative detection of OH radicals produced when H_2O is illuminated with 121.6 nm light from a hydrogen discharge source. The OH radicals so produced are in an excited electronic state, and relax via emission of a photon at 309 nm, which is detected with a photomultiplier. The H_2O concentration is proportional to the concentration of OH radicals detected after correcting for effects of scattering, and absorption by O_2 (primarily a problem in the troposphere). Frost point hygrometers measure dew point directly

by employing some technique for monitoring condensation on a surface. Chilled-mirror hygrometers use the attenuation of an optical beam reflected from a temperature-controlled mirror to indicate that condensation has occurred, and the temperature of the mirror at this point is the dew point. In another variation, a surface acoustic wave (SAW) device is employed (*Hoenk*, 1997) which displays a characteristic frequency response when water (or some other substance) condenses on the surface of the device. Frost point hygrometers generally have a slow time response (seconds), but do provide a direct measurement of dew point which can be converted to H_2O partial pressure (or volume mixing ratio) with a knowledge of total pressure.

There is a long history of atmospheric H_2O measurements from the ER-2 aircraft by researchers at the NOAA Aeronomy Laboratory [*Kley et al.*, 1983; *Kelly et al.*, 1990, 1991, 1993; *Rosenlof et al.*, 1997]. More recently, *Wennberg et al.* [1994] at Harvard University developed a state-of-the-art instrument for stratospheric measurements of OH and HO_2, which also contains a package for measurements of water vapor using the Lyman-α technique [*Weinstock et al.*, 1994; *Hintsa et al*, 1994]. There are also active H_2O measurement programs utilizing the NASA DC-8 aircraft (*Newell et al.*, 1996a), and balloon platforms [*Hofmann et al.*, 1991; *Oltmans and Hofmann*, 1995], which provide additional measurements of water vapor in the upper troposphere and stratosphere. Satellite measurements from the Halogen Occultation experiment (HALOE) [*Russell et al.*, 1993; *Harries et al.*, 1996; *Remsberg et al.*, 1996], the Stratospheric Aerosol and Gas Experiment (SAGE), [*McCormick et al.*, 1993; *Chiou et al.*, 1993], the Limb Infrared Monitor of the Stratosphere (LIMS) [*Gille and Russell*, 1984; *Russell et al.*, 1984], the Microwave Limb Sounder (MLS) [*Read et al.*, 1995; *Newell et al.*, 1996b], and shuttle measurements from the Atmospheric Trace Molecule Spectroscopy experiment (ATMOS) [*Rinsland et al.*, 1996, *Abbas et al.*, 1996] have also provided a wealth of information on the global distributions of H_2O in the stratosphere and upper troposphere. Only a few of the more recent references are listed here, but the measurement history of H_2O in the atmosphere is extensive. However, there is often disagreement among measurements of water vapor made by different techniques, even from the same platform, and improved techniques for *in-situ* measurements are needed.

This paper reports the results of a program initiated at JPL in 1992 to develop high-quality distributed feedback (DFB) diode lasers specifically for use in atmospheric spectrometers. Because it was recognized that in, principle, an open-path external optical absorption path provides the most simple and direct *in-situ* measurement possible, especially for water vapor, maintaining stability and alignment of an external multipass mirror arrangement over the wide temperature and pressure ranges expected was a significant component of the program. Initial target wavelengths for the lasers were 1.37 μm for H_2O, 1.43 and 2.05 μm for CO_2, and 1.65 μm for CH_4. By 1994 excellent single-frequency (DFB) devices operating at each of these selected wavelengths were produced, and new electronic circuit designs for laser control and signal processing were developed. In 1995 a compact, lightweight instrument was built for mounting on aircraft platforms (NASA ER-2 or NCAR WB57F). In mid-1996 this instrument underwent initial test flights on the ER-2, and in the fall of 1996 a series of engineering and calibration flights were undertaken. The instrument is now science-flight ready and provided stratospheric water vapor measurements as part of the NASA POLARIS (Photochemistry of Ozone Loss in the Arctic Region In Summer) ER-2 mission operating from sites in Alaska (Fairbanks) and Hawaii (Barbers Point) during the period April - September, 1997.

2. Instrument Description

Optical System

Figure 1 shows the basic layout of the instrument whose primary feature is an open-path, multipass "Herriott" cell [*Herriott et al.*, 1964; *Altmann et al.*, 1981] mounted external to the aircraft in "clean" air outside of the aircraft boundary layer. The boundary layer thickens with distance aft along the aircraft structure. In the present case, interference from airflow along the fuselage itself is not a concern because the superpod is located far enough out on the right wing to be unaffected by the fuselage streamlines. Also, the mounting location on the right wing superpod is forward of the leading edge of the wing so that only airflow along the superpod itself influences the H_2O measurements. This mounting location required the optical path to be >2" away from the superpod skin to clear the boundary layer. The entire optical path is located a minimum of 2.25" from the superpod skin, with the Herriott cell optical axis being located at a distance of 3.75" below the superpod skin. Laser light is directed into the multipass cell directly after collimation with no additional beam steering optics, and the exit beam from the cell impinges upon an InGaAs detector located adjacent to the laser in an evacuated optical housing. The optical housing is also mounted external to the aircraft directly behind the Herriott cell coupling mirror. The total optical path within the evacuated optical housing is <1 cm, which eliminates any residual H_2O absorption which could add uncertainty to the measurement. Total instrument weight, in flight-ready condition, is 8.2 kg including power supplies, cabling, and insulation.

The Herriott cell consists of two zerodur mirrors with identical focal lengths of 109.83 mm, and diameter 63.5 mm. A chromium-gold primary coating with an Al_2O_3 protective overcoat has proven to be very durable with little loss of reflectivity at 1.37 μm even after >30 flights on the ER-2. The mirror spacing is 20.61 cm, which corresponds to a 54-pass system and a total optical absorption pathlength of 11.13 m. Each mirror is mounted in an elliptically-profiled holder with a 6.66:1 major:minor axis ratio. This ensures nearly-laminar flow across the mirror surfaces and minimizes beam jitter at the detector caused by turbulent air flow in the region between the Herriott cell mirrors (especially near the mirror surfaces). Small (5W) heaters are attached to the back of each mirror to prevent condensation on aircraft descent from the cold stratosphere.

An angled Al mount holds the laser package (standard 9-mm TO "can") at the appropriate Herriott cell injection angle (6.65 degrees in both X and Y, relative to the optical axis of the Herriott cell), as well as the collimating lens (4.5 mm diameter asphere, 4.5 mm focal length), and a 3-mm active area InGaAs detector. The laser/detector separation is a function of distance from the Herriott cell coupling mirror as determined by the composite angle between the entrance and exit beams. A 15mm x 15mm, 3W, thermoelectric cooler (TEC) is sandwiched between the Al laser mount and a second Al disk which serves as the "sink" for the TEC. The temperature of this Al sink is held at a predefined temperature (nominally 15 C, set via software) during flights using a pulse-width-modulated (PWM) control loop. The TEC therefore operates as a cooler or a heater as required, but draws little power since the Al sink is always held close to the desired stabilization temperature of the TDL. Both the laser and detector temperatures are held constant within $\pm$0.01K during flights.

Electronics

Second harmonic detection is implemented for the near-IR spectrometer, as was used with the BLISS [*Webster and May*, 1987; *Webster et al.*, 1990], ALIAS [*Webster et al.*, 1994) and ALIAS-II [*Scott et al.*, 1997] mid-IR spectrometers developed within our group at JPL. However, control of the TDL current scan waveform is based on a new scheme involving an audio codec integrated circuit (IC) and PC-AT bus interface. Details of the second harmonic detection technique, and data interpretation methods, can be found in *Webster et al.*, 1988 and *May and Webster*, 1993. Briefly, a constant-period sawtooth current ramp is applied to the TDL to scan the output wavelength over the desired spectral interval (typically 1-3 cm^{-1}). A small-amplitude sinusoidal waveform at frequency f is added to the ramp, and the detector signal is demodulated at 2f to produce the second harmonic spectrum. The amplitude of the sinusoidal modulation is adjusted to produce the optimum 2f spectrum based on the conditions of the measurement. Since the molecular line shape varies with pressure and temperature, some care is required in choosing the optimum modulation amplitude if its value is not continually updated by the software based upon current pressure and temperature measurements. For the instrument configuration described here the laser scan ramp rate is fixed at 10 Hz, the laser modulation frequency is 10 KHz (2f detection frequency 20 KHz) and the modulation amplitude is held fixed at a value optimum for approximately 80 mbar pressure.

Control of the laser current scan waveform is accomplished by using the audio codec (Crystal Semiconductor CS4215) in continuous DMA mode. The codec has two 16-bit digital-to-analog (D/A) converters, and two 16-bit analog-to-digital (A/D) converters on board, as well as programmable attenuation on the D/A outputs, programmable gain on the A/D inputs, and sophisticated digital filtering. Figure 2 shows a block diagram of the electronics configuration with the codec interfaced to a standard PC-AT bus via an interface IC (Crystal Semiconductor CS4131). The laser scan waveform (ramp plus sine wave) is generated in a software array at program initialization, and continuously output via 16-bit DMA to the laser drive circuitry. Demodulator phase is controlled by shifting the sine wave in the frequency domain when the software scan array is generated. Once the system is started the laser scan waveform is continuously output to the laser drive circuitry. The demodulator reference frequency, which is generated using the second digital-to-analog output provided by the codec, is simultaneously output to the demodulator circuitry. Transmission (dc) and second harmonic (2f) spectra are acquired using the two A/D input channels on the codec. Since the codec sampling rate is fixed, both the D/A and the A/D channels are updated at the same rates, resulting in significant oversampling of the A/D. However, aside from excess use of system RAM, there is no penalty incurred from oversampling the spectrum.

The electronics boards are all PC104 format and operate from +5 VDC and +12VDC provided by converting the aircraft 400 Hz, 120 VAC power to 28 VDC. This base 28 VDC is used directly for structural heater control, and down-converted to +5V and +12V using DC-DC converter modules (Vicor Corp). Five boards comprise the PC104 "stack." A video controller board is present for operation in the laboratory where spectra are displayed along with instrument parameters and housekeeping data. Calibration and flight data are stored on a 40 MB ATA flash card inserted into a PCMCIA adapter board which fits onto the PC104 stack. The computer board (Ampro Corp.) contains an 80486Dxi microprocessor running at 100 MHz, along with standard serial and parallel ports. A serial port is wired to an external connector on the aircraft

mounting hatch and used to communicate with a laptop computer for preflight instrument setup and operational checks. The remaining two boards are custom designs.

One custom board controls the laser and performs the 2f signal processing (primary board), as just described. A second custom board (secondary board) provides three channels of pulse-width-modulated (PWM) heater control, and five channels of 16-bit A/D conversion along with conditioning circuitry for standard thermistors. The PWM control circuits switch 28V from the main system power supply to strip heaters (Minco) chosen according to the desired wattage. Total power consumption for the electronics, excluding the structural heaters, is 7.5W. The structural heater power varies from zero when the aircraft is on the ground (preflight checks and taxi) to approximately 90W for the coldest atmospheric conditions (temperatures as low as 190K have been observed at the troposphere in the tropics). The Al box surrounding the electronics has an O-ring seal and the inside of the box is maintained at 1 atm pressure during flights. Although this provision is not strictly necessary, the small size of the enclosure makes it simple to provide this seal, and because the main baseplate is also temperature stabilized using one of the PWM control circuits, component temperature drift and overheating (especially of the CPU chip) are minimized.

Software

A master C++ program (MS-DOS executable) configures the hardware and operates the spectrometer in a continuous data acquisition mode. After initialization of the hardware an infinite loop is initiated where three logical flags are used to control the program sequencing. Each flag corresponds to a specific operational mode. These modes are *FLIGHT*, *GROUND*, and *TEST* corresponding to flight operation, operation in the laboratory (used primarily for setup), and a non-graphical (command-line) test mode.

A command parser accepts user commands in *GROUND* and *TEST* modes. All instrument parameters can be modified and stored via keyboard commands. Laser scan parameters, dc and 2f gains (provided by the codec), and demodulator phase setting are the most common adjustments (for example, these are necessary whenever a new laser is installed or a new scan region is desired). Provisions also exist for saving individual spectral scans to the flash card, calibrating the electronics response, and changing the basic signal integration time by changing the number of scans averaged to produce each spectrum that will be processed.

Preliminary gas concentrations are calculated "on-the-fly" by the software using the algorithms described by *May and Webster*, 1993. A matrix of synthetic 2f signal amplitudes for a fixed volume mixing ratio is calculated on a predefined grid in pressure (40-1040 mbar) and temperature (180 - 320K). Based on the electronics calibrations, the experimental 2f signal amplitude at a given atmospheric pressure and temperature is converted to spectroscopic units and compared to the synthetic 2f amplitude, whose value is determined by interpolation on the 2-D synthetic matrix.

3. Calibration and Data Analysis

Calibration consists of first measuring the spectral line parameters that are necessary to apply the Beer-Lambert law relating observed line center absorption to absorber number density,

$$\rho = \frac{-\ln[\tau(\nu)]}{k(\nu)L} \tag{1}$$

where ρ is the absorber number density, $\tau(\nu)$ is the observed transmission at wavenumber ν, and L is the optical pathlength. $k(\nu)$ is the absorption coefficient and requires knowledge of the line strength and molecular line shape for the transition of interest;

$$k(\nu) = \frac{S}{\gamma_d}\left(\frac{\ln 2}{\pi}\right)^{1/2} V(x,y) \tag{2}$$

S is the line strength, γ_d is the Doppler half-width-at-half-maximum (HWHM), and V(x,y) is the Voigt line shape function

$$V(x,y) = \frac{y}{\pi}\int_0^\infty \frac{e^{-t^2}}{y^2 + (x-t)^2}dt \tag{3}$$

parameterized by x and y,

$$x = \left(\frac{\nu - \nu_o}{\gamma_d}\right)(\ln 2)^{1/2} \tag{4}$$

$$y = \left(\frac{\gamma_L}{\gamma_d}\right)(\ln 2)^{1/2} \tag{5}$$

ν_o is the wavenumber at line center, and γ_L is the Lorentz HWHM resulting from collisional line broadening. γ_L has a temperature dependence which is generally modeled as

$$\gamma_L(T) = \gamma_L(T_o)\left(\frac{T_o}{T}\right)^n \tag{6}$$

where T_o is a reference temperature, and n ranges typically from 0.5 to 1.0, with n = 0.75 being characteristic of most molecular transitions based on laboratory measurements. For open-path measurements in the upper troposphere and stratosphere, knowledge of γ_L and its dependence on temperature are critical.

For increased detection sensitivity second harmonic detection [*May and Webster*, 1993] is utilized in which a small-amplitude sinusoidal modulation is added to the base sawtooth laser current scan ramp. The detector signal is demodulated at twice the sine wave frequency to produce second harmonic lineshapes. The second harmonic signal amplitude is given by,

$$H_2 = C \int_{-\pi}^{\pi} V[x(\Theta), y]\cos(2\Theta)d\Theta \qquad (7)$$

where x is now a function of theta due to the sinusoidal modulation placed on the laser scan waveform, and C is a constant. To quantify an observed 2f spectral line the amplitude of the sine wave modulation must also be known precisely. Techniques for determining the modulation amplitude are described by *May and Webster*, 1993.

Assuming the spectral line parameters, their temperature dependence, and the modulation amplitude are known, a data processing matrix can be derived based on Eqn. 7. For a fixed modulation amplitude H_2 is evaluated on predefined grids in temperature and pressure that cover the possible values encountered during an aircraft flight. For the ER-2 suitable ranges for temperature and pressure are 180 - 320 K, and 40 - 1040 mbar, respectively. An example of such a matrix is shown in Fig. 3 calculated for a fixed volume mixing ratio for H_2O of 5 ppmv, and grid step sizes of 5 K in temperature and 10 mbar in pressure. When the line center absorption is sufficiently low that the approximation $e^{-x} \sim 1-x$ is valid, Eqn. 1 reduces to a linear dependence of absorber number density on line center absorption. The observed 2f signal amplitudes can then be converted to spectroscopic units and linearly scaled to the data processing matrix entries to obtain the measured volume mixing ratio [*May and Webster*, 1993]. For larger line center absorption values the correct logarithmic relationship from Eqn. 1 is required, and the dc spectra must be analyzed to determine the equivalent unmodulated line center absorption for correct scaling of the data processing matrix entries. With an optical pathlength of 11.13 m, the line center absorption for 5 ppmv H_2O in the stratosphere is <1%, so errors from linearly scaling to the data processing matrix are negligible. In the upper troposphere the line center absorption values can be considerably larger, and eventually saturate above about 400 ppmv for a pathlength of 11.13 m. When the line center absorption is significant (but below saturation) the mixing ratio obtained by linearly scaling to the data processing entries must be multiplied by the ratio $e^{-A_o}/(1-A_o)$, where $A_o = 1-\tau(\nu_o)$ is the absorption at line center, to properly apply Eqn. 1. This process requires conversion of the observed modulated direct absorption level to the appropriate unmodulated value, as illustrated in Fig. 4.

For laboratory spectroscopic measurements, and calibrations using standard gas mixtures, a thermal-vacuum chamber was constructed which is controllable in temperature from ambient down to 220 K, and in pressure from ambient down to $<10^{-3}$ Torr, to simulate the atmospheric conditions of a typical ER-2 flight. The entire H_2O instrument fits into the chamber and can be operated in a continuous data acquisition mode where spectra are written to the flash card at predetermined intervals. Standard calibration gas mixtures can also be admitted to the chamber, or flowed through it. When operating in a flowing mode at ambient temperatures, a chilled mirror hygrometer (General Eastern model 1311DR) is placed in the flow stream on the exit of the chamber to monitor the water vapor partial pressure in the stream. Standard mixtures of H_2O in air were purchased from Air Liquide Corp. with stated assay accuracies of 2%. Measurements using the General Eastern hygrometer directly at the cylinder regulator outputs showed the assays to be within $\pm$1.5 ppmv at nominal 52 ppmv mixtures. Instrument response measurements using these gas mixtures were carried out to confirm the line strength and air-broadening values determined from extensive laboratory studies of the H_2O line at 7294.1229 cm^{-1}, and to evaluate the data processing algorithms developed for handling flight data.

The line strength for the target H_2O line was measured using pure distilled H_2O in a continuous flow system. While notoriously difficult to eliminate from a vacuum system at room temperatures, a continuous flow system using pure H_2O vapor is ideal for line strength measurements since it is a stable gas that does not react or break down. A capacitance manometer with a 0 - 1 Torr head, attached at the center of a 39.61 cm long single-pass absorption cell, provided pressure measurements. Flow rate was controlled using a stainless-steel needle valve, and measurements were made over a pressure range of 50 - 400 mTorr so that self-broadening was minimal. Figure 5a shows a Doppler-limited spectrum and a least squares fit using Eqn. 2 with V(x,y) replaced with a Gaussian appropriate for the low-pressure lineshapes. The laser linewidth was also determined from the fits and was represented well with a Gaussian (HWHM 62 MHz) to within the standard deviation of the fits. Extensive measurements yielded a 296 K line strength of 1.55×10^{-20} cm^{-1}/cm^{-2}-molecule with a standard deviation in the measurements of 0.9%. Considering uncertainties in the pressure and temperature measurements, and the standard deviation of the individual fits, the estimated uncertainty in the measured line strength is $\pm$3%. The value 1.55×10^{-20} cm^{-1}/cm^{-2}-molecule is within 2% of the value derived by *Toth* [1994] from Fourier transform measurements (1.53×10^{-20} cm^{-1}/cm^{-2}-molecule). It also agrees with the values obtained using the standard gas mixtures to within 10%, although these measurements were not as reliable due to the large volume of the calibration chamber and the consequent difficulty in eliminating residual H_2O.

Air-broadening coefficients were measured using the standard gas mixtures, random mixtures where the chamber was purged using "zero" air, and actual flight data from the ER-2. Fig. 5b shows an example air-broadened spectrum recorded in the calibration chamber, along with a least-squares fit to the line shape. In Fig. 6 the combined results of all the air-broadened measurements are shown for the 7294.1229 cm-1 H_2O line as a function of temperature. A line corresponding to n = 0.75 in Eqn. 6 is also shown. A 296 K air broadening coefficient of 0.117 $\pm$0.003 cm^{-1}/atm best fits the data, but there is a slight curvature to the data indicating that the simple power law dependence may not hold precisely for this spectral line. The increase in pressure-broadened line width as temperature decreases appears to be more rapid than predicted by Eqn. 6, and the dependence of γ_L on temperature shown in Fig. 6 was used to generate the data processing matrix for the POLARIS ER-2 flight data. Using the same spectrometer in an identical configuration for the laboratory measurements, and the aircraft flight measurements, minimizes systematic errors in the data analysis process.

4. Measurement Capability

In the troposphere H_2O volume mixing ratios vary from roughly 3% (corresponding to 100% relative humidity) at the surface, down to several hundred parts per million by volume (ppmv) in the upper troposphere. Water enters the stratosphere through the cold tropical tropopause, which traps most of it, producing low stratospheric abundances (near 5 ppmv), a fraction of which is produced from methane oxidation. The stratospheric concentration of water vapor is much less variable than other trace gases and generally fluctuates around a mean value of approximately 5 ppmv. Thus, a concentration range spanning four orders of magnitude must be accomodated to perform measurements from the earth's surface to the stratosphere. In its present configuration the ER-2 instrument is optimized for measurements of water vapor in the stratosphere, although volume mixing ratios as high as 400 ppmv can be monitored before the

spectral line begins to saturate due to excessive water vapor concentrations in the 11.13 m optical path. There is no inherent limitation to the range of H_2O mixing ratios that can be measured with an instrument of this type as long as the optical pathlength is short enough to prevent saturation of the absorption line.

Figure 7 shows data from a recent flight (May 2, 1997) of the ER-2 northwards out of Fairbanks, AK where a measurement precision of +0.05 ppmv for a two second integration time is demonstrated. This precision level is typically 4-5 times higher than Lyman-α spectrometers are able to obtain for daytime measurements for equivalent signal integration periods. In the stratosphere, preliminary comparisons show that the TDL measurements agree well with the Lyman-α measurements on the ER-2 in terms of absolute volume mixing ratios for H_2O. However, final data processing for the recently-completed POLARIS mission is not yet complete. On May 9, 1997 the ER-2 flew a pattern where the aircraft intercepted its own exhaust plume on several occasions (Fig. 8). Integration of the plume "spikes", and analysis of similar features in other gases measured on the ER-2 (CO, CO_2, NO, NO_y, particles) allows emission indices to be calculated for the ER-2 engine. Similar measurements are necessary to characterize exhausts for newly developed aircraft engines. *Fahey et al.* [1995a, 1995b] have carried out such analyses for previous wake encounters of the ER-2. In Fig. 9 a summary of stratospheric TDL H_2O measurements for eleven ER-2 flights from the first two legs of the POLARIS mission is shown. The tight correlation with the tracer N_2O, measured by the ALIAS instrument [*Webster et al.*, 1994], demonstrates consistency in the H_2O measurements with this new instrument, which performed reliably during the POLARIS mission. Intercomparisons with the Harvard H_2O instrument, and discussion of science results from the POLARIS mission, will be presented elsewhere.

5. Summary

An open-path near-infrared TDL spectrometer for atmospheric measurements of water vapor has been developed and flown successfully on the NASA ER-2 research aircraft. Measurement precision is higher than that of instruments using the Lyman-α technique due to the inherent advantage of a high-power (mW) mid-IR laser source, and insensitivity to scattered solar radiation. The technique of direct absorption spectroscopy using an open-path absorption cell also eliminates problems associated with wall reactions and sample extraction, it is a direct and noninvasive measurement of H_2O, and affords high-speed sampling independent of flow rate restrictions for studies requiring fast time response. A version of this instrument is currently being designed for simultaneous measurements of HDO and H_2O using a Pb-salt laser operating near 6.7 μm wavelength. Measurements of these isotopes of H_2O near the tropopause region should yield valuable insight into transport dynamics and stratosphere-troposphere exchange mechanisms.

Several improvements to the basic spectrometer design are currently being implemented based on experience gained during the POLARIS flight series. Chief among these is a change in the detection frequency from 20 KHz to 256 KHz using an analog circuit to generate the laser modulation. The limiting factor on in-flight signal-to-noise ratio was beam jitter at the detector caused by the high-speed air flow (200 m/s) between the Herriott cell mirrors. Calculations indicate that higher detection frequencies should help to minimize beam jitter noise, and higher frequency detection for TDL spectrometers, in general, is beneficial [*Bomse et al.*, 1992]. Flights

aboard the NASA WB57F aircraft based at Johnson Space Center in Houston, Texas, are scheduled for January 1998. A modified version of the instrument for tropospheric measurements is being built at JPL for flights on the NASA DC-8 aircraft as part of the Convection and Moisture Experiment (CAMEX-3) which will take place in the late summer of 1998 out of Patrick Air Force Base in Florida.

Acknowledgments. W. Steve Woodward of the University of North Carolina at Chapel Hill provided the circuit designs and example control software for the primary and secondary board circuits, and was tremendously valuable as always in all aspects of electrical engineering, circuit programming and tuning, and thermal analysis. Linley Kroll (JPL) provided the detailed mechanical engineering for this instrument. Special thanks to the ER-2 operations crew at NASA Ames, the POLARIS project scientists David Fahey and Paul Newman, and NASA Code Y UARP program manager Michael Kurylo, for supporting flights of this new instrument on the ER-2. This research described in this publication was carried out by the Jet Propulsion Laboratory, California Institute of Technology, under a contract with the National Aeronautics and Space Administration.

References

Abbas, M.M., H.A. Michelsen, M.R. Gunson, M.C. Abrams, M.J. Newchurch, R.J. Salawitch, A.Y. Chang, A. Goldman, F.W. Irion, G.L. Manney, E.J. Moyer, R. Nagaraju, C.P. Rinsland, G.P. Stiller, and R. Zander, Seasonal variations of water vapor in the lower stratosphere inferred from ATMOS/ATLAS 3 measurements of H_2O and CH_4, *Geophys. Res. Lett., 23*, 2401-2404, 1996.

Altmann, J., R. Baumgart, and D.C. Weitkamp, Two-mirror multipass absorption cell, *Appl. Opt., 20*, 995-999, 1981.

Bomse, D.A., A.C. Stanton, and J.A. Silver, Frequency modulation and wavelength modulation spectroscopies: comparison of experimental methods using a lead-salt diode laser, *Appl. Opt., 31*, 718-731, 1992.

Chiou, E.W., M.P. McCormick, L.R. McMaster, W.P. Chu, J.C. Larsen, D. Rind and S. Oltmans, Intercomparison of stratospheric water vapor observed by satellite experiments - stratospheric aerosol and gas experiment-II versus limb infrared monitor of the stratosphere and atmospheric trace molecule spectroscopy, *J. Geophys. Res., 98*, 4875-4887, 1993.

Fahey, D.W., E.R. Keim, E.L. Woodbridge, R.S. Gao, K.A. Boering, B.C. Daube, S.C. Wofsy, R.P. Lohmann, E.J. Hintsa, A.E. Dessler, C.R. Webster, R.D. May, C.A. Brock, J.C. Wilson, R.C. Miake-Lye, R.C. Brown, J.M. Rodriguez, M. Loewenstein, M.H. Proffitt, R.M. Stimpfle, S.W. Bowen, and K.R. Chan, In situ observations in aircraft exhaust plumes in the lower stratosphere at midlatitudes, *J. Geophys. Res, 100*, 3065-3074, 1995a.

Fahey, D.W., E.R. Keim, K.A. Boering, C.A. Brock, J.C. Wilson, H.H. Jonsson, S. Anthony, T.F. Hanisco, P.O. Wennberg, R.C. Miake-Lye, R.J. Salawitchm N. Louisnard, E.L. Woodbridge, R.S. Gao, S.G. Donnelly, R.C. Wamsley, L.A. Del Negro, S. Solomon, B.C. Daube, S.C. Wofsy, C.R. Webster, R.D. May, K.K. Kelly, M. Loewenstein, J.R. Podolske, and K.R. Chan, Emission measurements of the Concorde supersonic aircraft in the lower stratosphere, *Science, 270*, 70-74, 1995b.

Gille, J.C. and J.M. Russell, The limb infrared monitor of the stratosphere: experiment performance, and results, *J. Geophys. Res., 89*, 5125-5140, 1984.

Harries, J.E., J.M. Russell, A.F. Tuck, L.L. Gordley, P. Purcell, K. Stone, R.M. Bevilacqua, M.R. Gunson, G. Nedoluha and W. Traub, Validation of measurements of water vapor from the halogen occultation experiment (HALOE), *J. Geophys. Res., 101,* 10205-10216, 1996.

Herriott, D.R., H. Kogelnik, and R. Kompfner, Off-axis paths in spherical mirror resonators, *Appl. Opt., 3*, 523-526, 1964.

Hintsa, E.J., E.M. Weinstock, A.E. Dessler, J.G. Anderson, M. Loewenstein and J.R. Podolske, SPADE H_2O measurements and the seasonal cycle of stratospheric water vapor, *Geophys. Res. Lett., 21*, 2559-2562, 1994.

Hoenk, M.E., G. Cardell, D. Price, R.K. Watson, T.R. VanZandt, D.Y. Cheng, W.J. Kaiser, Surface acoustic wave microhygrometer, SAE Technical Paper Series, paper #972393 (1997)..

Hofmann, D.J., S.J. Oltmans and T. Deshler, Simultaneous balloon-borne measurements of stratospheric water vapor and ozone, *Geophys. Res. Lett., 18*, 1011-1014, 1991.

Jones, R.L. and J.F.B. Mitchell, Is water vapour understood?, *Nature, 353*, 210, 1991.

Kelly, K.K., A.F. Tuck, L.E. Heidt, M. Loewenstein, J.R. Podolske, S.E. Strahan and J.F. Vedder, A comparison of ER-2 measurements of stratospheric water vapor between the 1987 antarctic and 1989 arctic airborne missions, *Geophys. Res. Lett., 17*, 465-468, 1990.

Kelly, K.K., A.F. Tuck, and T. Davies, Wintertime asymmetry of upper tropospheric water between the northern and southern hemispheres, *Nature, 353*, 244-247, 1991.

Kelly, K.K., M.H. Proffitt, K.R. Chan, M. Loewenstein, J.R. Podolske, S.E. Strahan, J.C. Wilson and D. Kley, Water vapor and cloud water measurements over Darwin during the STEP 1987 tropical mission, *J. Geophys. Res., 98,* 8713-8723, 1993.

Kley, D.A., A. Schmeltekopf, K. Kelly, R. Winkler, T. Thompson, and M. McFarland, The U-2 Lyman-alpha results from the 1980 Panana Experiment; the 1980 Stratospheric-Tropospheric Exchange Experiment, Ed: A.P. Margozzi, *NASA Technical Memorandum 94297*, U.S. Government Printing Office, Washington, D.C.

Manabe, S. and R.T. Wetherald, Thermal equilibrium of the atmosphere with a given distribution of relative humidity, *J. Atmos. Sci., 24*, 241-259, 1967.

May, R.D., and C.R. Webster, Data processing and calibration for tunable diode laser harmonic absorption spectrometers, *J. Quant. Spectrosc. Radiat. Transfer, 49*, 335-347, 1993.

McCormick, M.P., E.W. Chiou, L.R. McMaster, W.P. Chu, J.C. Larsen, D. Rind and S. Oltmans, Annual variations of water-vapor in the stratosphere and upper troposphere observed by the stratospheric aerosol and gas experiment-II water-vapor retrieval, *J. Geophys. Res., 98*, 4867-4874, 1993.

Newell, R.E., Y. Zhu, E.V. Browell, S. Ismail, W.G. Read, J.W. Waters, K.K. Kelly, and S.C. liu, Upper-tropospheric water vapor and cirrus - comparison of DC-8 observations, preliminary UARS microwave limb sounder measurements, and meterological analyses, *J. Geophys. Res., 101*, 1931-1941, 1996a.

Newell, R.E., Y. Zhu, E.V. Browell, W.G. Read, and J.W. Waters, Walker circulation and tropical upper tropospheric water vapor, *J. Geophys. Res., 101*, 1931-1941, 1996b.

Oltmans, S.J., and D.J. Hofmann, Increase in lower-stratospheric water-vapor at a mid-latitude northern-hemisphere site from 1981 to 1994, *Nature, 374*, 146-149, 1995.

Read, W.G., J.W. Waters, D.A. Flower, L. Froidevaux, R.F. Jarnot, D.L. Hartmann, R.S. Harwood, and R.B. Hood, Upper-tropospheric water vapor from UARS MLS, *Bull. Amer. Metero. Soc., 76*, 2381-2389, 1995.

Remsberg, E.E., P.P. Bhatt, and J.M. Russell, Estimates of the water vapor budget of the stratosphere from UARS HALOE data, *J. Geophys. Res., 101*, 6749-6766, 1996.

Rinsland, C.P., M.R. Gunson, R.J. Salawitch, M.J. Newchurch, R. Zander, M.M. Abbas, M.C. Abrams, G.L. Manney, H.A. Michelsen, A.Y. Chang, and A. Goldman, ATMOS measurements of H_2O + CH_4 and total reactive nitrogen in the November 1994 Antarctic stratosphere: Dehydration and denitrification in the vortex, *Geophys. Res. Lett., 23*, 2397-2400, 1996.

Rosenlof, K.H., K.K. Kelly, J.M. Russell, and M.P. McCormick, Hemispheric asymmetries in water-vapor and inferences about transport in the lower stratosphere, *J. Geophys. Res, 102*, 13213-13234, 1997.

Russell, J.M., J.C. Gille, E.E. Remsberg, L.L. Gordley, P.L. Bailey, H. Fischer, A. Girard, S.R. Drayson, W. Evans and J.E. Harries, Validation of water vapor results measure by the Limb Infrared Monitor of the Stratosphere experiment on Nimbus 7, *J. Geophys. Res., 89*, 5115-5124, 1984.

Russell, J.M., L.L. Gordley, J.H. Park, S.R. Drayson, W.D. Hesketh, R.J. Cicerone, A.F. Tuck, J.E. Frederick, J.E. Harries and P.J. Crutzen, The halogen occultation experiment, *J. Geophys. Res., 98,* 10777-10797, 1993.

Scott, D.C., R.H. Herman, C.R. Webster, R.D. May, G. Flesch, and W.S. Woodward, Aircraft Laser Infrared Absorption Spectrometer II (ALIAS-II) for in-situ atmospheric measurements of N_2O and CH_4 (*in preparation*).

Toth, R.A., Extensive measurements of $H_2{}^{16}O$ line frequencies and strengths: 5750 to 7965 cm-1, *Appl. Opt., 33*, 4851-4867, 1994.

Webster, C.R., R.T. Menzies, and E.D. Hinkley, Infrared laser absorption: theory and applications, in *Laser Remote Chemical Analysis*, Chapter 3, edited by R.M. Measures, John Wiley, New York, 1988.

Webster, C.R. and R.D. May, Simultaneous *in situ* measurements and diurnal variations of NO, NO_2, O_3, jNO_2, CH_4, H_2O, and CO_2 in the 40 to 26 km region using an open path tunable diode laser spectrometer, *J. Geophys. Res., 92*, 11931-11950, 1987.

Webster, C.R., R.D. May, R. Toumi, and J.A. Pyle, Active nitrogen partitioning and the nighttime formation of N_2O_5 in the stratosphere: simultaneous *in situ* measurements of NO, NO_2, HNO_3, O_3, and N_2O using the BLISS diode laser spectrometer, *J. Geophys. Res., 95*, 13851-13866, 1990.

Webster, C.R., R.D. May, C.A. Trimble, R.A. Chave, and J. Kendall, Aircraft (ER-2) laser infrared absorption spectrometer (ALIAS) for *in-situ* stratospheric measurements of HCl, N_2O, CH_4, NO_2, and HNO_3, *Appl. Opt., 33*, 454-472, 1994.

Weinstock, E.M., E.J. Hintsa, A.E. Dessler, J.F. Oliver, N.L. Hazen, J.N. Demusz, N.T. Allen, L.B. Lapson and J.G. Anderson, A new fast response photofragment fluorescence hygrometer for use on the NASA ER-2 and Perseus remotely-piloted aircraft, *Rev. Sci. Instrum. 65*, 3544-3554, 1994.

Wennberg, P.O., R.C. Cohen, N.L. Hazen, L.B. Lapson, N.T. Allen, T.F. Hanisco, J.F. Oliver, N.W. Lanham, J.N. Demusz, and J.G. Anderson, Aircraft-borne, laser-induced fluorescence instrument for the in situ detection of hydroxyl and hydroperoxyl radicals, *Rev. Sci. Instrum., 65*, 1858-1876, 1994.

Figure Captions

1. Instrument location on the ER-2 (left) and assembly for mounting in a camera port in the right wing superpod (right). A two-piece assembly made of G-10 material is used to mount the instrument electronics and optical systems. The main section of this assembly is a circular plate, 16.8" in diameter, that is profiled around the edge to fit within the camera port cutout in the superpod. It is held in place with a retaining ring and a rubber gasket during flights. The electronics and power supply module are mounted on an aluminum baseplate that is attached to the inboard side of the circular G-10 plate as shown. In the center of the main G-10 plate is a rectangular cutout which holds a separate G-10 optics mounting plate. The optical head and Herriott cell mirrors are mounted to the rectangular plate, which drops into the cutout with 0.030" clearance on all sides to mechanically isolate it from the circular plate. The optics mounting plate is held in place with teflon strips and a screw-down assembly that allows the main circular plate to flex or contract thermally without affecting the alignment of the Herriott cell. Three thin invar rods keep the Herriott cell mirror separation stable during the large temperature changes encountered during flights.

2. Block diagram of the laser control and signal processing electronics. The laser scan waveform is continually played out to the drive circuitry via 16-bit DMA, and spectra are continuously read in via a second DMA channel. An audio codec integrated circuit is at the heart of the system. A secondary board contains three pulse-width-modulation drive signals, and five analog-to-digital (A/D) channels for monitoring ambient air temperature and pressure. Two of the A/Dchannels are used to monitor the ambient air temperature and pressure, and the remaining three channels accept thermistor inputs used for the structural heater control loops.

3. Example of a synthetic data processing matrix calculated using Eqn. 7. These matrices are generally defined over a pressure range of 40 - 1040 mbar, but since water vapor concentrations are too high in the lower troposphere for the optical pathlength chosen for ER-2 measurements, the matrix has been cut off at 500 mbar. The modulation amplitude used to generate this matrix was fixed, so that at higher pressures the spectral line is undermodulated relative to the value which produces the largest amplitude 2f signal. The rapid increase in the peak-to-peak 2f signal amplitude (pp2f) with decreasing temperature is due to the low ground state energy for the spectral line at 7294.1229 cm^{-1} (E" = 23.8 cm^{-1}).

4. Illustration of the effects of laser wavelength modulation on the direct transmission spectral line shape. Although the area under the spectral line is conserved, the sinusoidal modulation broadens the line and, for sufficiently large modulation amplitude, causes a dip in the center. This dip is due to the fact that the sinusoidal waveform, over one period of its oscillation (corresponding to the integration limits in Eqn. 7), occupies more time at the extremes than at the center and therefore samples regions on the wings of the spectral line where the absorption is small. For Beer-Lambert law corrections, the true (unmodulated) line center transmission value must be extracted from the modulated transmission spectrum, which is recorded by the DC spectrum channel during flights.

5. Examples of Doppler-limited (a) and air-broadened (b) laboratory spectra used to determine the spectral line parameters and their temperature dependence. Peak-to-peak residuals (observed - calculated) from least squares fits were typically 0.6% of the line center absorption ($1 - \tau(\nu_o)$) value. Approximately 1000 spectra were recorded operating the spectrometer in a continuous data acquisition mode in the calibration chamber to derive the air-broadening coefficient and its dependence on temperature for the target spectral line.

6. Results of extensive air-broadening measurements for the 7294.1229 cm^{-1} line of H_2O. The red line is a quadratic fit to the data, and the green line corresponds to n = 0.75 in Eqn. 6. The log of the measured broadening coefficient ratio is plotted against the log of the temperature ratio which should, according to Eqn. 6, produce a straight line with a slope equal to n. The curvature observed appears to be real and indicates a more rapid increase in the air-broadening coefficient than predicted by the simple power law relationship of Eqn. 6.

7. ER-2 data from a flight north out of Fairbanks, AK on May 2, 1997. The noise level in the data is $\pm$ 0.05 ppmv for a 2 s spectrum integration time (ie. 20 spectra averaged to produce each data point). The low H_2O values seen near the beginning (hygropause on ascent), middle (ER-2 "dive" to 50,000 feet at the north end of the flight track), and end (hygropause on descent) of the plot reflect a typical ER-2 flight profile.

8. ER-2 data from a "racetrack" type flight track where the ER-2 repeatedly crossed its own exhaust wake. The sharp spikes upward in the data correcpond to wake crossing events, and the spectrum integration time was reduced to 1 s to obtain better resolution for these encounters. Analysis of such measurments for H_2O, and other gases measured on the ER-2, provides emission indices for the aircraft engine and is useful for characterizing the potential impact of aircraft emissions on climate.

9. Summary of ER-2 data for the first eleven flights of the POLARIS mission. H_2O data are plotted against ALIAS measurements of N_2O to illustrate the consistent performance of the instrument on a flight-to-flight basis. Note the extremely low levels of N_2O observed during the early stages of the mission, and consequent high (6 ppmv) values of H_2O. The ER-2 encountered air masses which had decsended from much higher altitudes in the northern polar region. Since H_2O is formed in the stratosphere by oxidation of CH_4, older air from higher altitudes contains higher volume mixing ratios of H_2O.

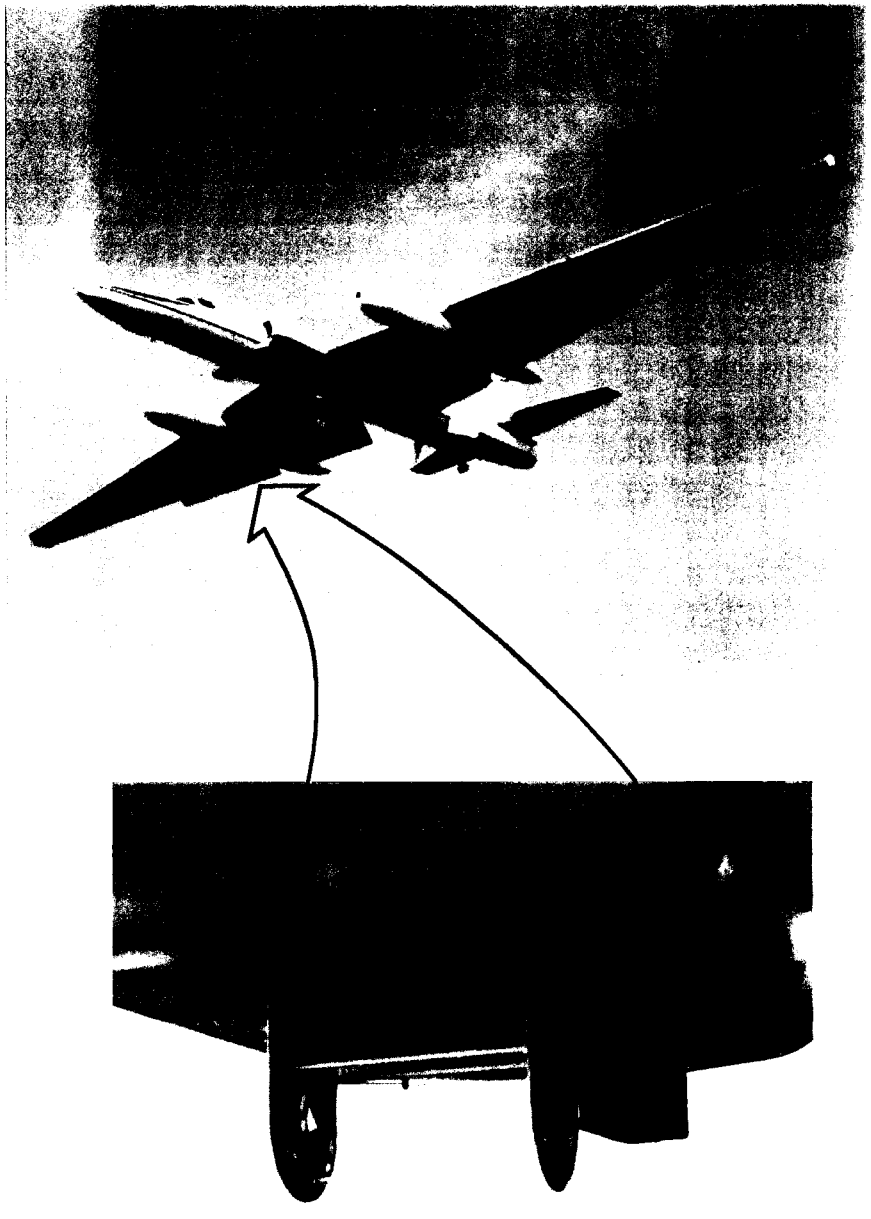

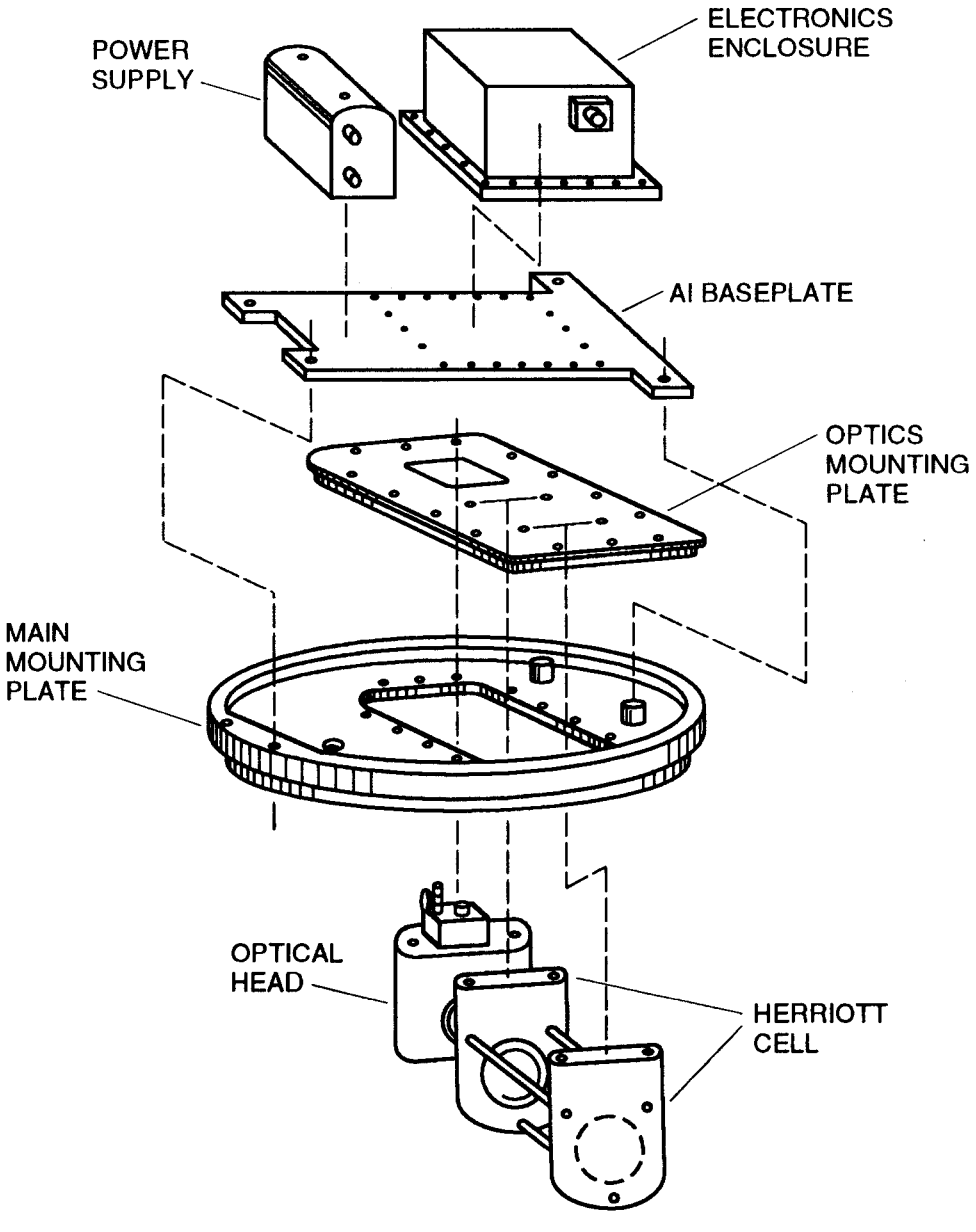
ELECTRONICS ENCLOSURE
POWER SUPPLY
Al BASEPLATE
OPTICS MOUNTING PLATE
MAIN MOUNTING PLATE
OPTICAL HEAD
HERRIOTT CELL

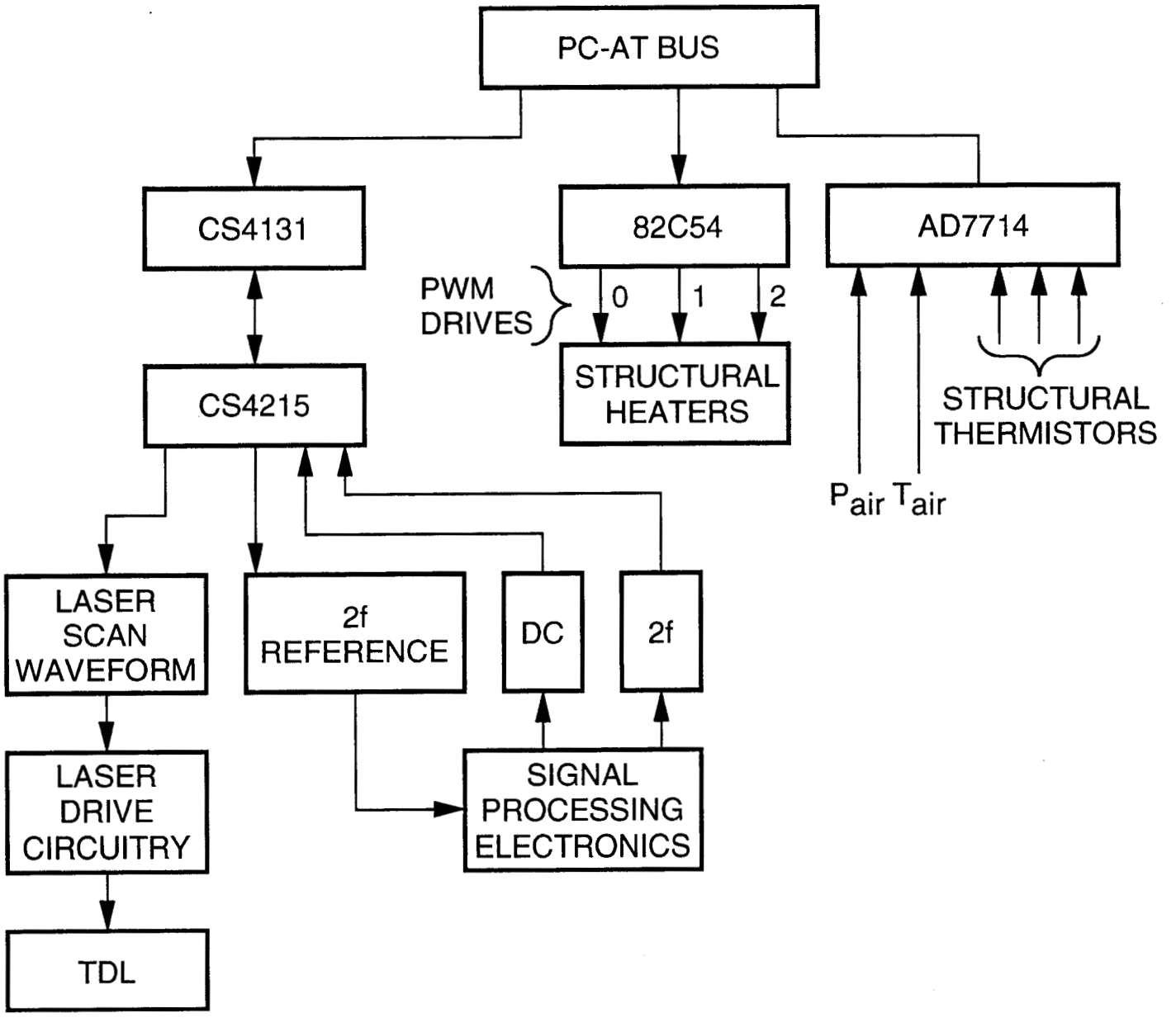
PC-AT BUS
CS4131
82C54
AD7714
PWM
DRIVES
0
1
2
STRUCTURAL
HEATERS
CS4215
STRUCTURAL
THERMISTORS
Pair Tair
LASER
SCAN
WAVEFORM
2f
REFERENCE
DC
2f
LASER
DRIVE
CIRCUITRY
SIGNAL
PROCESSING
ELECTRONICS
TDL

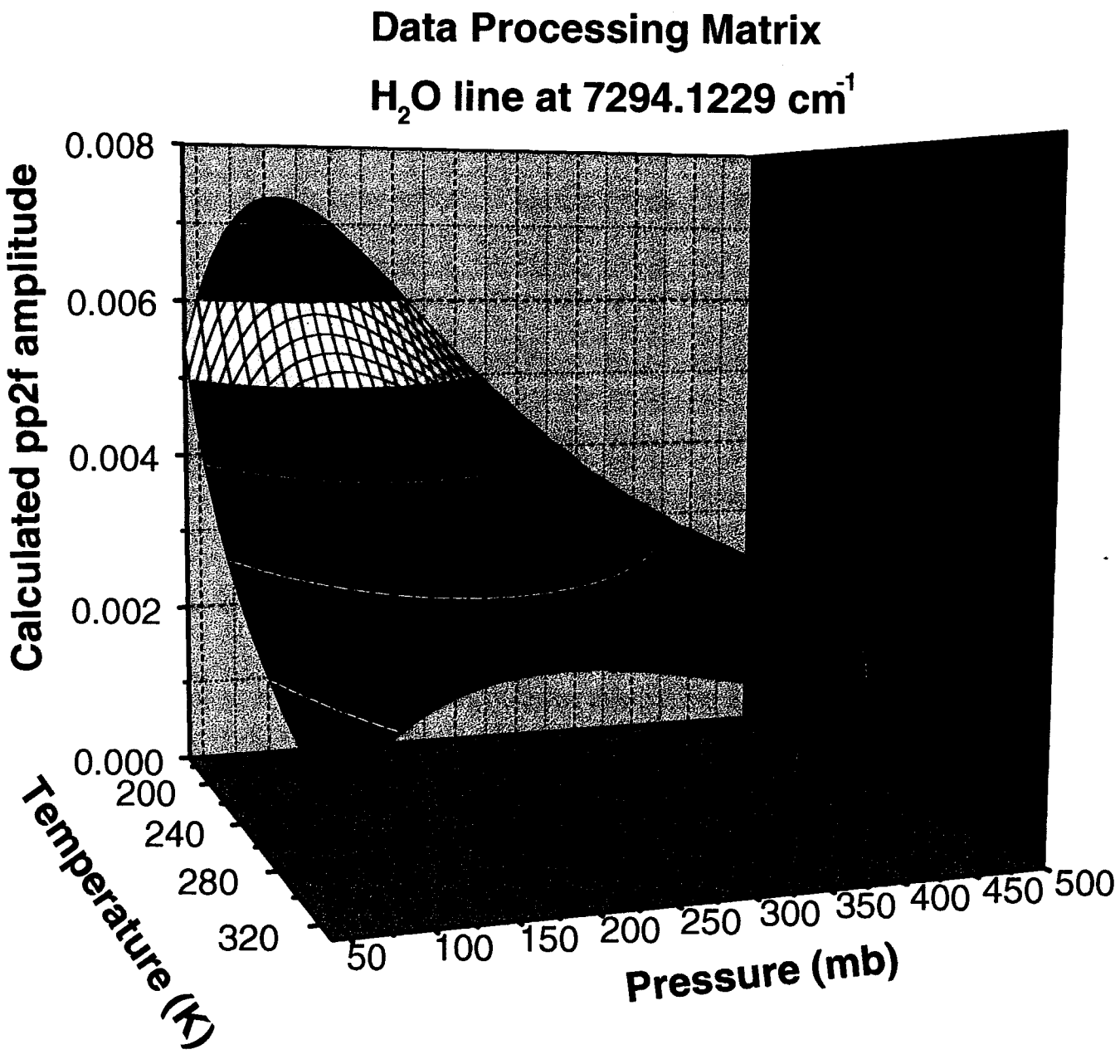
Data Processing Matrix
H2O line at 7294.1229 cm-1
Calculated pp2f amplitude
0.008
0.006
0.004
0.002
0.000
Temperature (K)
200
240
280
320
Pressure (mb)
50
100
150
200
250
300
350
400
450
500

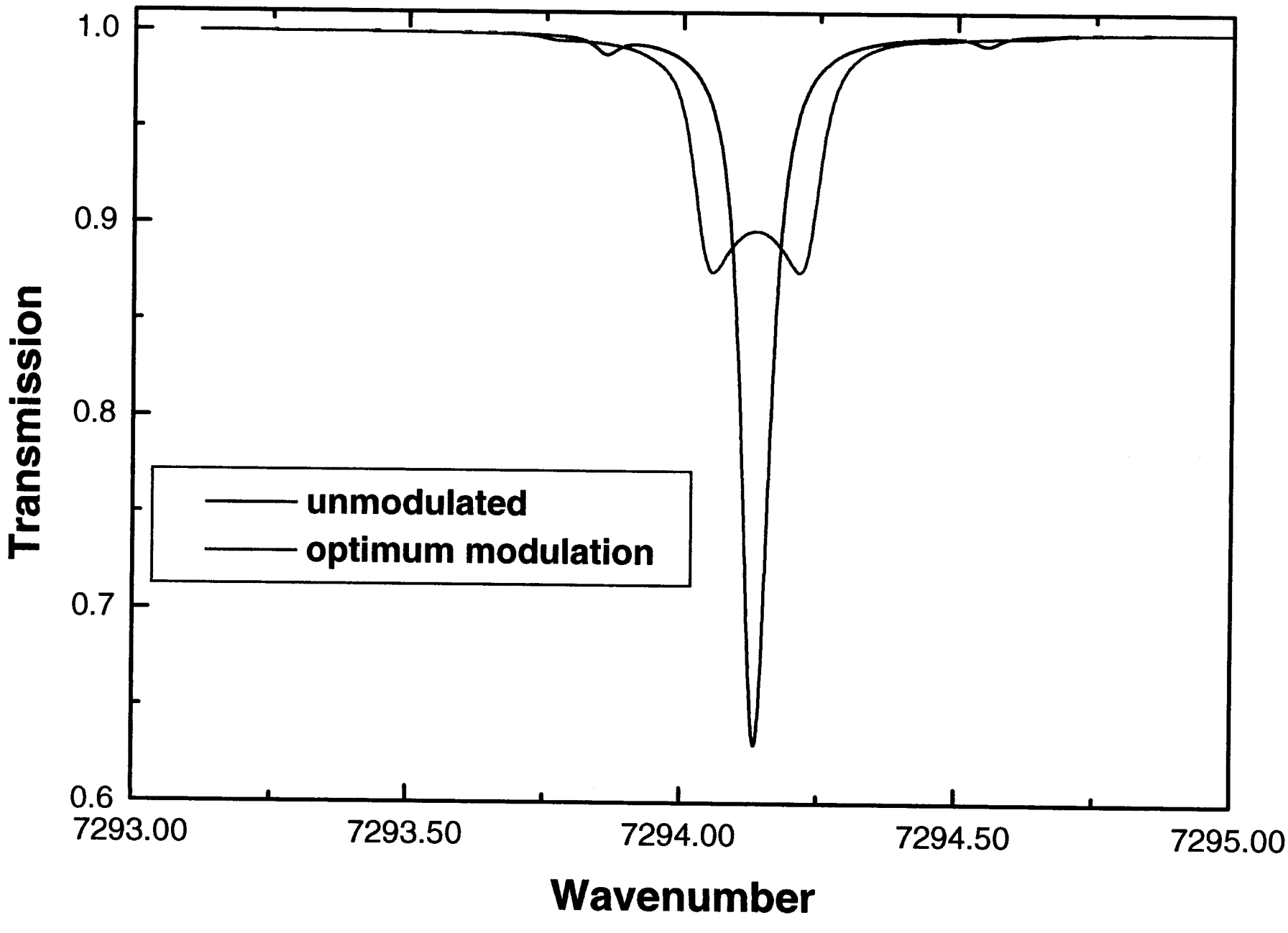
1.0
0.9
0.8
0.7
0.6
Transmission
unmodulated
optimum modulation
7293.00
7293.50
7294.00
7294.50
7295.00
Wavenumber

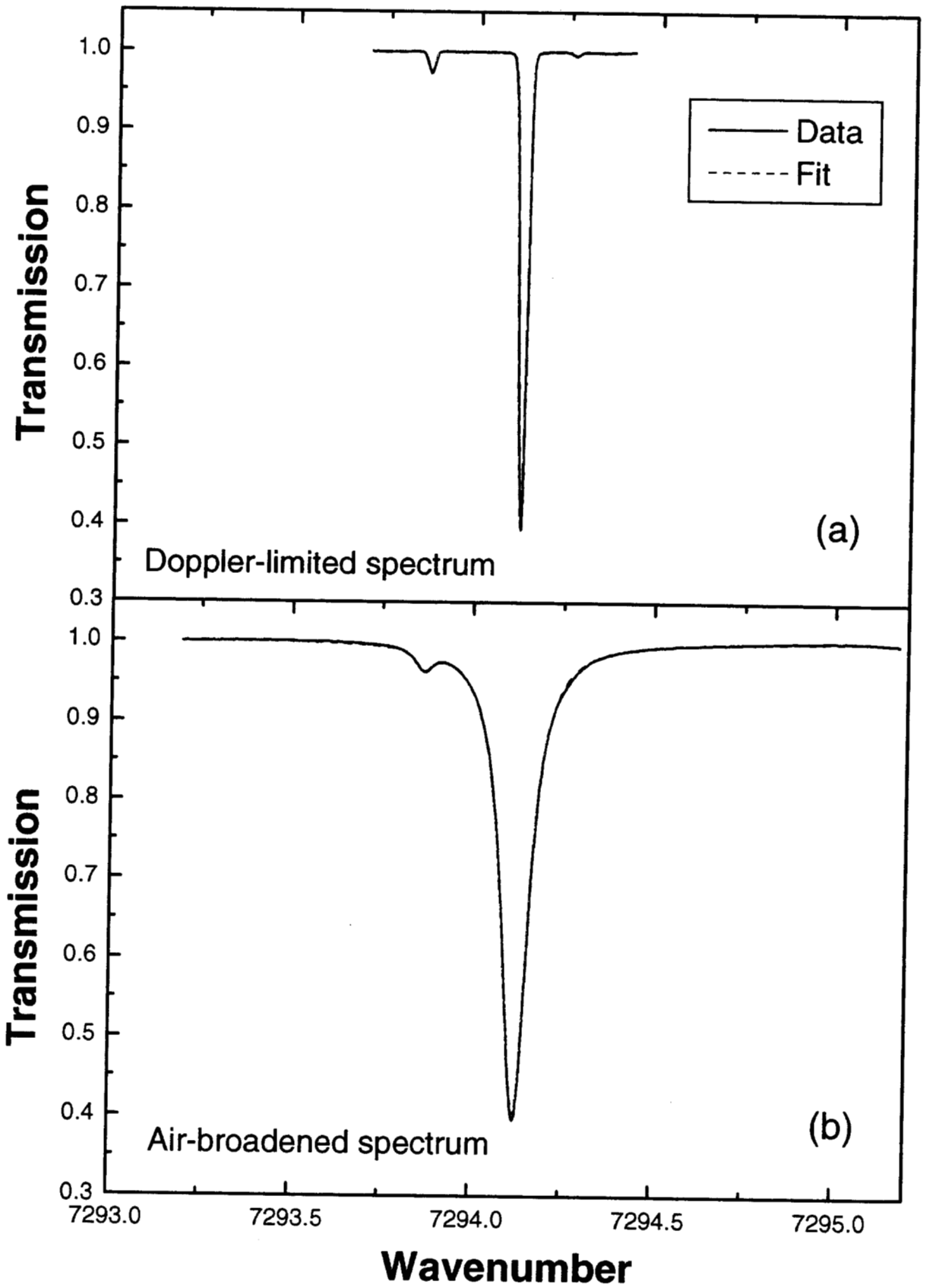
Transmission
1.0
0.9
0.8
0.7
0.6
0.5
0.4
0.3
Data
Fit
(a)
Doppler-limited spectrum
Transmission
1.0
0.9
0.8
0.7
0.6
0.5
0.4
0.3
(b)
Air-broadened spectrum
7293.0
7293.5
7294.0
7294.5
7295.0
Wavenumber

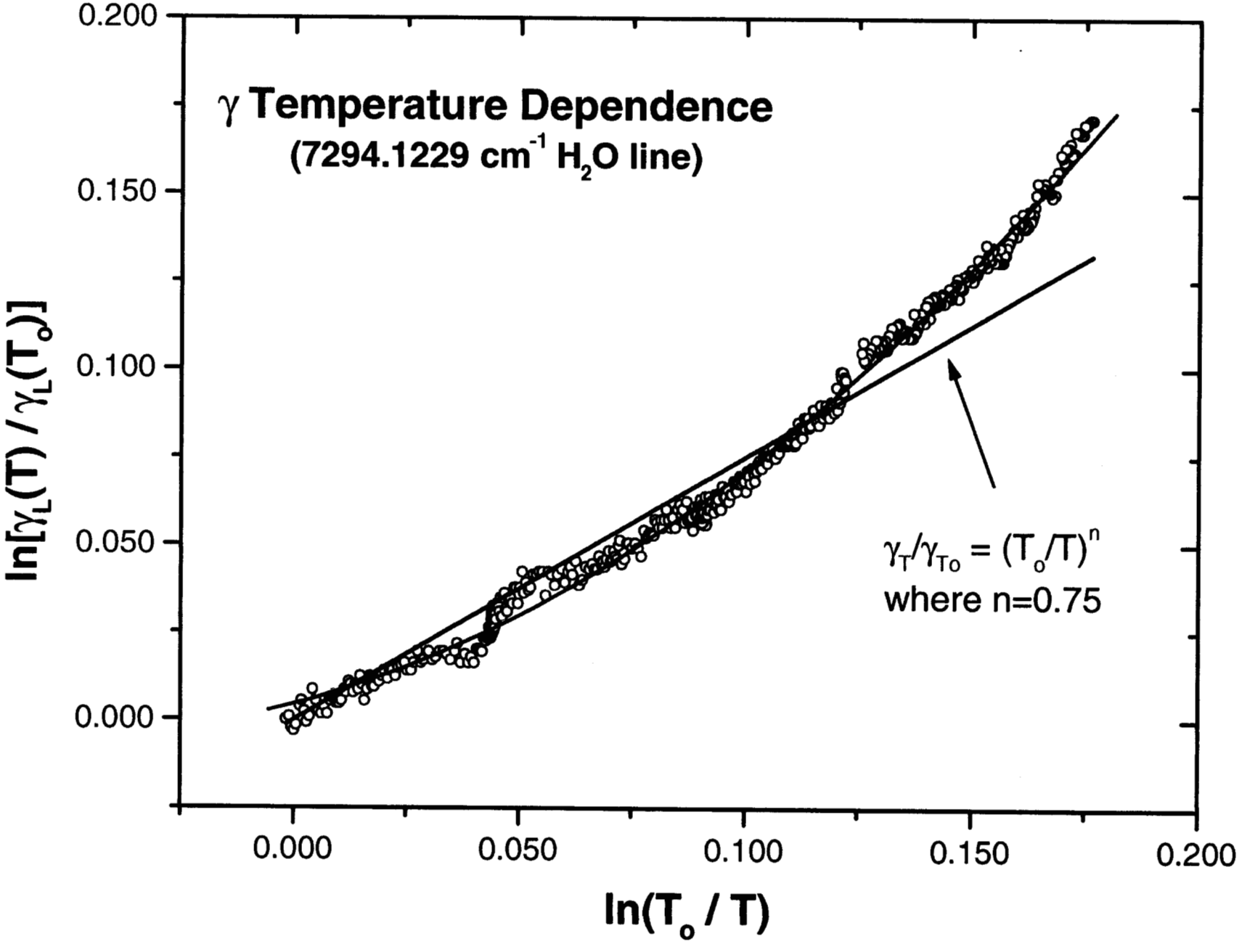
γ Temperature Dependence
(7294.1229 cm-1 H2O line)
ln[γL(T) / γL(To)]
ln(To / T)
γT/γTo = (To/T)n
where n=0.75
0.200
0.150
0.100
0.050
0.000
0.000
0.050
0.100
0.150
0.200

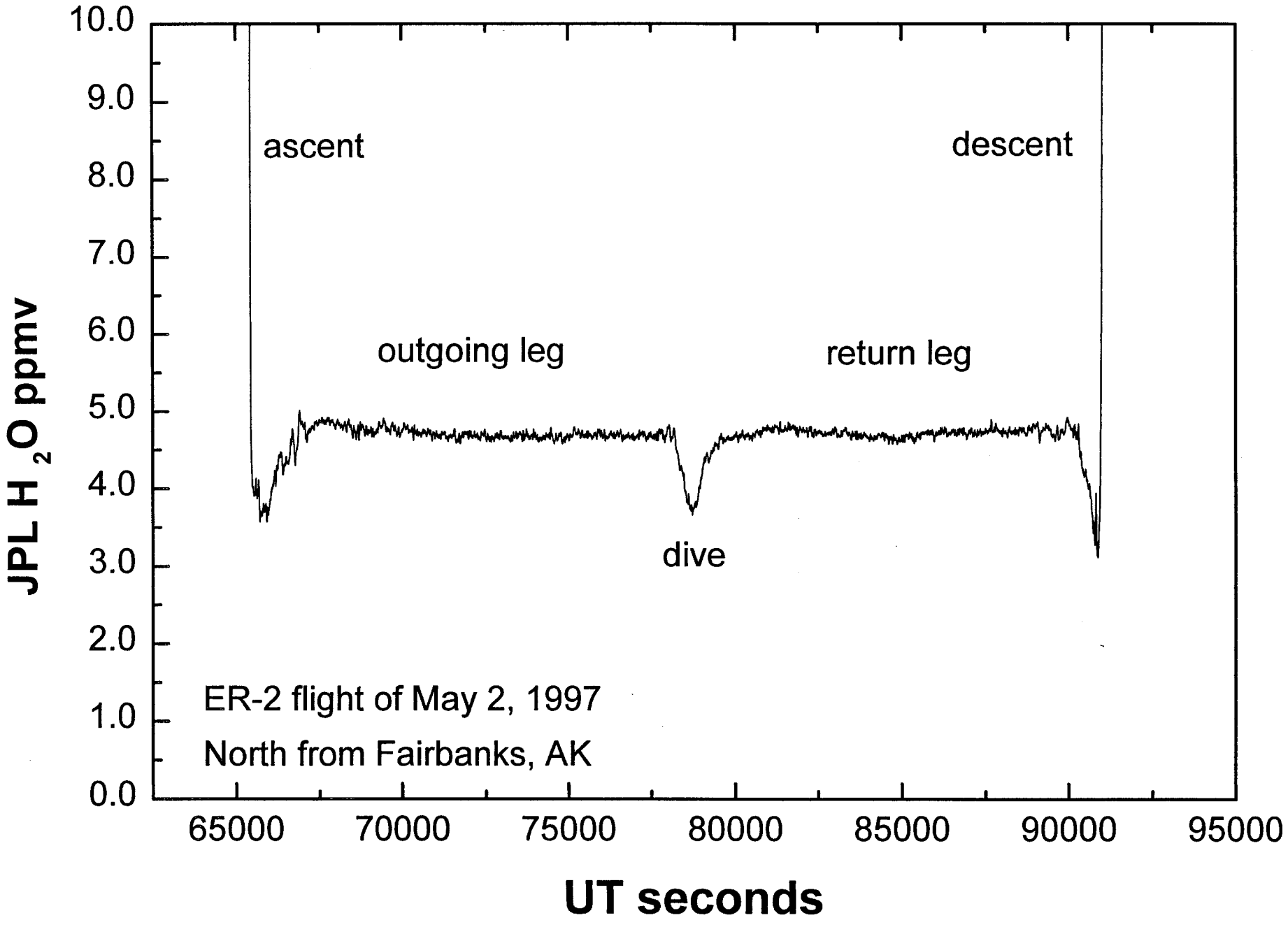
10.0
9.0
8.0
7.0
6.0
5.0
4.0
3.0
2.0
1.0
0.0
JPL H 2O ppmv
ascent
descent
outgoing leg
return leg
dive
ER-2 flight of May 2, 1997
North from Fairbanks, AK
65000
70000
75000
80000
85000
90000
95000
UT seconds

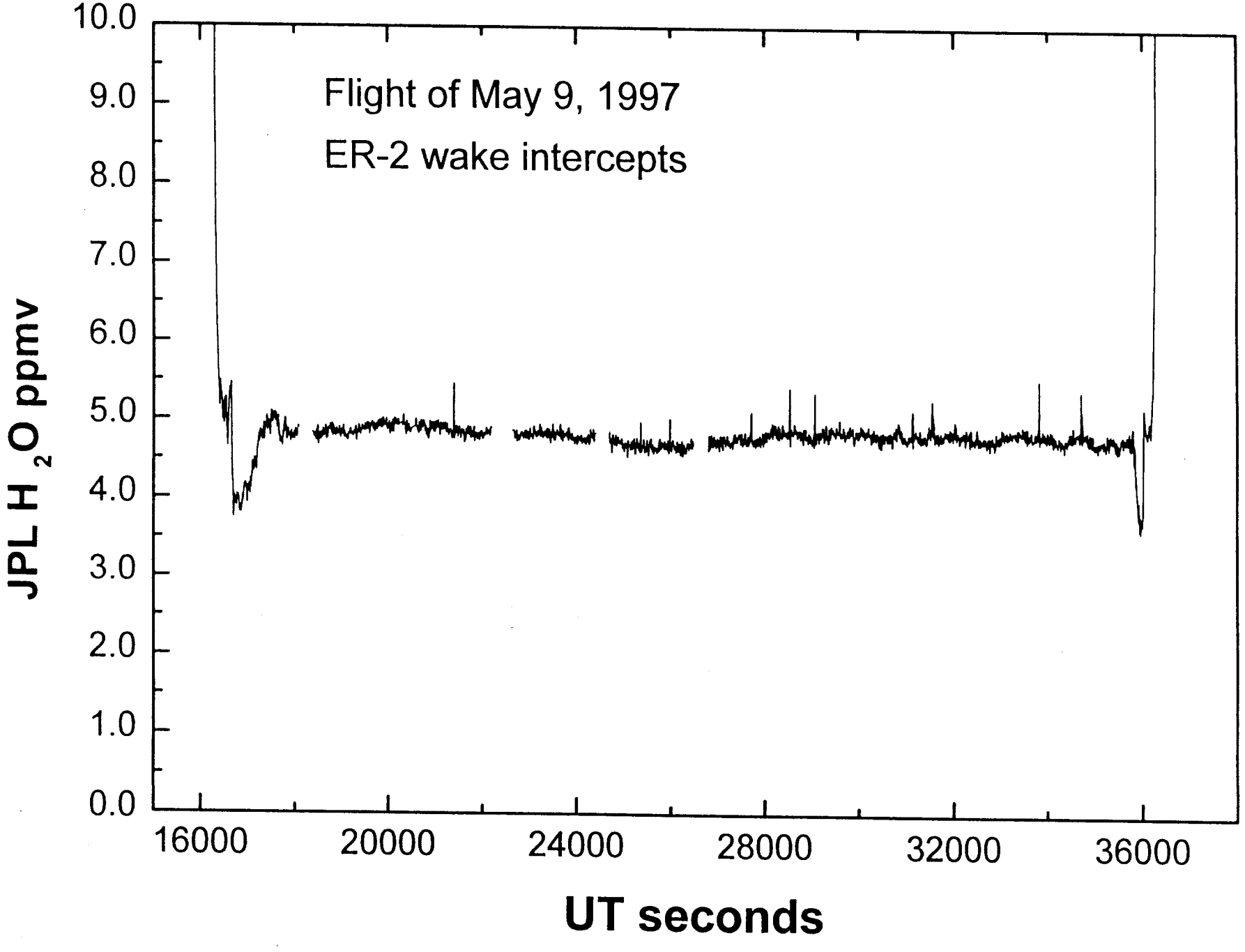
Flight of May 9, 1997
ER-2 wake intercepts
JPL H 2O ppmv
10.0
9.0
8.0
7.0
6.0
5.0
4.0
3.0
2.0
1.0
0.0
16000
20000
24000
28000
32000
36000
UT seconds

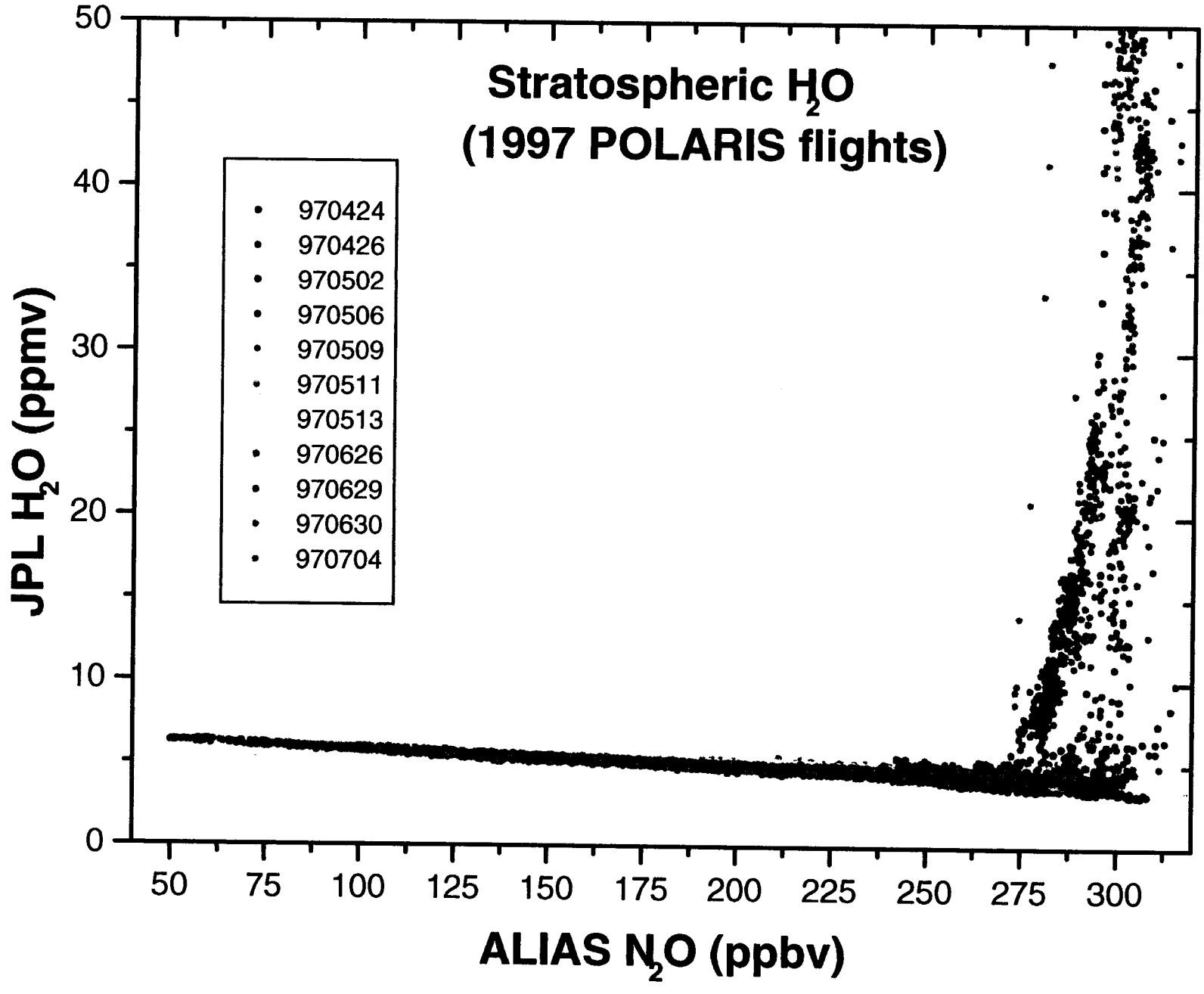
Stratospheric H2O
(1997 POLARIS flights)
970424
970426
970502
970506
970509
970511
970513
970626
970629
970630
970704
JPL H2O (ppmv)
ALIAS N2O (ppbv)
0
10
20
30
40
50
50
75
100
125
150
175
200
225
250
275
300